

pynasonde — Methods & API Reference

Technical guide for ionospheric researchers

pynasonde Development Team

Version 1.0 — March 28, 2026

Contents

1	Architecture Overview	1
1.1	Published v1.0 architecture	1
1.2	Complete file-format and class index	2
2	Instrument Overview	3
2.1	VIPIR	3
2.2	DIGISONDE DPS4D	3
3	VIPIR Echo Extraction & Filtering	5
3.1	Seven-parameter echo extraction	5
4	Capon Cross-Spectrum Es Layer Imaging	6
4.1	Physical motivation	6
4.2	Hankel subband matrix and covariance	6
4.3	Capon pseudospectrum	7
4.4	Singularity constraints	7
5	Multi-File A+B+C Combining (RiqAggregator)	8
5.1	Combining strategy	8
6	HF Radio Absorption	8
7	True Height Inversion	9
8	Polarization & Spread-F	10
9	Ionospheric Irregularity Analysis	10
9.1	Physical motivation	10
9.2	Structure function approach	11
9.3	Height-resolved and anisotropy analysis	11
10	NeXtYZ 3-D Electron Density Inversion	11
10.1	Wedge-Stratified Ionosphere model	11
10.2	Hamiltonian eikonal ray tracing	12
10.3	Inversion loop	12

11 API Quick-Reference	12
11.1 All public imports	12
11.2 Constructor summary	13
11.3 Result dataclasses at a glance	14

Abstract

pynasonde is an open-source Python toolkit for reading, analysing, and visualising ionosonde data from both **VIPiR** and **DIGISONDE DPS4D** instruments. This document gives the mathematical foundations for each analysis algorithm, the design rationale behind key implementation choices, and a compact API cheat-sheet. Target audience: researchers who want to understand the algorithms, extend the toolkit, or apply it to new data sets.

Published reference: Chakraborty S., Bullett T., Barjatya A., Mabie J. (2026). pynasonde: An open-source Python library for ionosonde data processing. *SoftwareX* 34, 102617. <https://doi.org/10.1016/j.softx.2026.102617>

1 Architecture Overview

1.1 Published v1.0 architecture

The library is organised into two instrument modules (**digisonde** and **vipir**) each with dedicated parsers and plotting routines, plus a new cross-instrument analysis layer added after publication.

Figure 2 of the SoftwareX paper shows the two-module architecture (digisonde, vipir) with colour-coded data types and plotting methods. The analysis layer described here is new post-publication.

1.2 Complete file-format and class index

Table 1: All supported file formats, parser classes, and primary methods. **[new]** = added after SoftwareX publication.

Extension	Type	Class	Primary methods / output
<i>DIGISONDE DPS4D</i>			
.SAO 4.3	ASCII	SaoExtractor	load_SAO_files() with height_profile or scaled_params
.SAO 5.0	XML	SaoExtractor	same API; SaoSummaryPlots.plot_TS()
.RSF	Binary	RsfExtractor	plot_direction_ionogram(), plot_directogram() [new]
.SBF	Binary	SbfExtractor	extract(), ionogram()
.DFT	ASCII	DftExtractor	plot_doppler_waterfall(), plot_doppler_spectra() [new]
.DVL	ASCII	DvlExtractor	load_DVL_files(), plot_dvl_drift_velocities()
.SKY	ASCII	SkyExtractor	extract(), to_pandas(), multi- panel plot_skymap()
.EDP	ASCII	EdpExtractor	extract(), electron density pro- file
<i>VIPIR</i>			
.RIQ	Binary	RiqDataset	create_from_file(), SCT + PCT, VIPIR_VERSION_MAP
.RIQ	—	EchoExtractor [new]	7-param Dynasonde echoes (h, A, V*, EP, PP, XL, YL)
.RIQ	—	IonogramFilter [new]	6-stage filter: RFI, EP, multi-hop, DBSCAN, RANSAC, temporal
.NGI	NetCDF	DataSource	load(), multi-file data cube ag- gregation
.NGI	—	AutoScaler	noise profiling, segmentation, bi- nary trace extraction
<i>Analysis layer (all new post-v1.0)</i>			
—	—	PolarizationClassifier	O/X mode separation via PP; hemisphere-aware
—	—	TrueHeightInversion	Titheridge/POLAN lamination; EDPResult
—	—	AbsorptionAnalyzer	LOF, O/X differential, calibrated, $\kappa(z)$
—	—	SpreadFAnalyzer	Range / frequency / mixed spread-F classification
—	—	IrregularityAnalyzer	EP structure function $\rightarrow \alpha(h)$, outer scale, anisotropy
—	—	IonogramScaler	foF2, foE, h'F, MUF from O- mode trace
—	—	EsCaponImager	Capon cross-spectrum, $\Delta r =$ r_0/K
—	—	RiqAggregator	Multi-file A+B+C, ~ 24 dB SNR gain
—	—	NeXtYZInverter	WSI model + Hamiltonian ray- tracing, 3-D $N(h, x, y)$
—	—	FullPipeline	End-to-end RIQ \rightarrow N(h) automa- tion

2 Instrument Overview

2.1 VIPIR

VIPIR (Vertical Incidence Pulsed Ionospheric Radar) records raw in-phase and quadrature (IQ) samples in binary .RIQ files. Each file contains a Sounding Control Table (SCT) followed by one Pulse Configuration Table (PCT) record per transmitted pulse. The IQ cube for one sounding frequency has shape (pulse_count, gate_count, rx_count).

Listing 1: VIPIR — load a RIQ file

```
from pynasonde.vipir.riq.parsers.read_riq import RiqDataset,
    VIPIR_VERSION_MAP

riq = RiqDataset.create_from_file(
    "data/WI937_20220821.RIQ",
    vipir_config=VIPIR_VERSION_MAP.configs[1], # data_type=1 (older
    format)
)
sct = riq.sct # SoundingControlTable
# Key fields: sct.timing.gate_count, sct.timing.gate_step (us),
#             sct.station.rx_count, sct.station.rx_position
```

WI937 (Wallops Island) pulses/freq, 960 gates (r₀ = 1.499 km), 8 Rx PL407 (Prudhoe Bay) format, data_type=2.

2.2 DIGISONDE DPS4D

The Digisonde DPS4D family stores data in several formats:

Extension	Class	Contents
.SAO	SaoExtractor	Scaled parameters (foF2, hmF2, MUF) + N(h) profile
.RSF	RsfExtractor	Raw amplitude + phase per frequency/height/azimuth
.SBF	SbfExtractor	Binary raw sounding (alternative to RSF)
.DFT	DftExtractor	Per-height Doppler spectra (velocity vs. height)
.DVL	DvlExtractor	Drift velocity estimates (V _x , V _y , V _z)
.SKY	SkyExtractor	Sky map (polar arrival-direction map)

SAO is the primary product for most science applications. RSF/SBF give access to amplitude and phase. DFT contains the full Doppler spectrum per height.

Listing 2: DIGISONDE — load SAO files in parallel

```
from pynasonde.digisonde.parsers.sao import SaoExtractor

df = SaoExtractor.load_SAO_files(
    folders=["data/KR835/"],
    func_name="height_profile", # or "scaled_params"
    n_procs=4,
)
# df columns: datetime, height_km, plasma_freq_mhz,
#             electron_density_cm3, ...
```

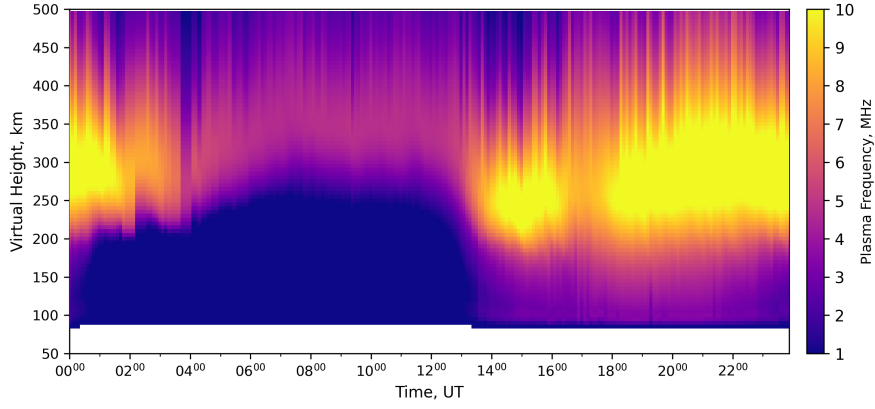


Figure 1: Daily isodensity contour from DPS4D SAO files at KR835. Each column is one $N(h)$ profile; colour encodes electron density (cm^{-3} , log scale).

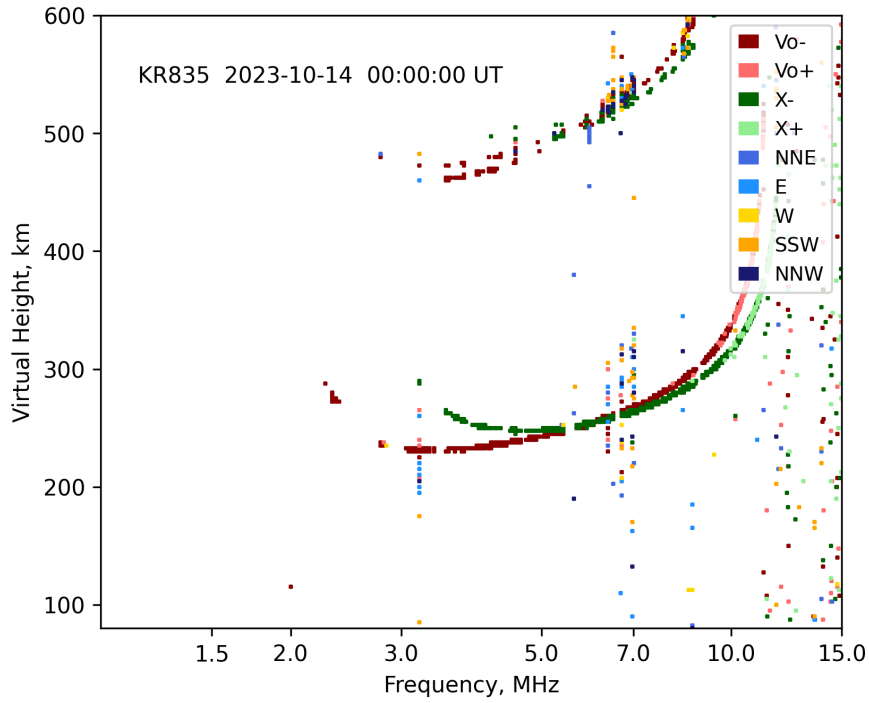


Figure 2: Direction-coded ionogram from a DPS4D RSF sounding at KR835. Colour encodes the echo arrival azimuth.

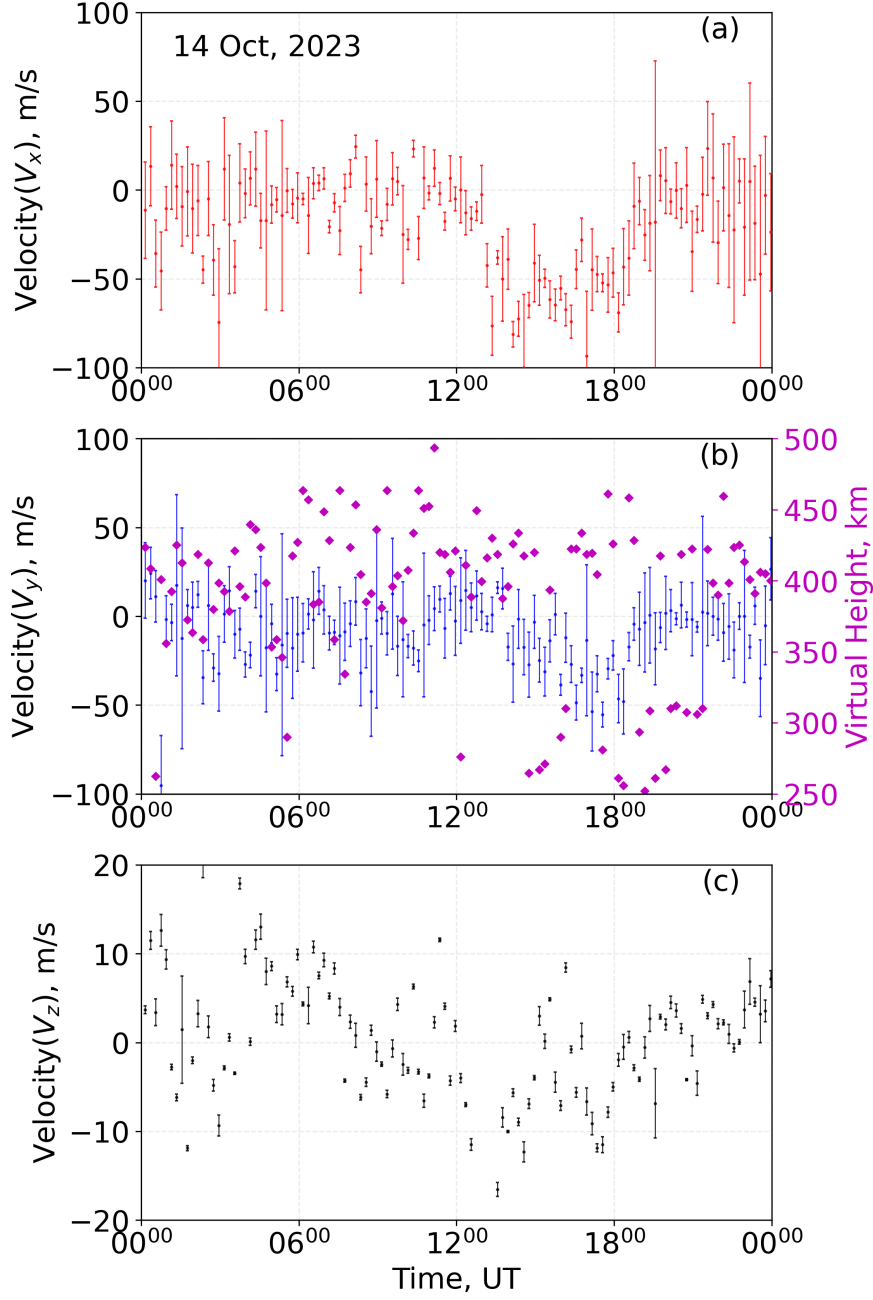


Figure 3: Three-panel drift velocity stack plot from DPS4D DVL files. Panels: V_x (east), V_y (north), V_z (vertical), with virtual-height overlay.

3 VIPIR Echo Extraction & Filtering

3.1 Seven-parameter echo extraction

`EchoExtractor` computes the seven Dynasonde-style echo parameters — height, amplitude, Doppler velocity V^* , wavefront residual EP, polarization chirality PP, and direction cosines XL/YL — from the pulse-compressed IQ cube.

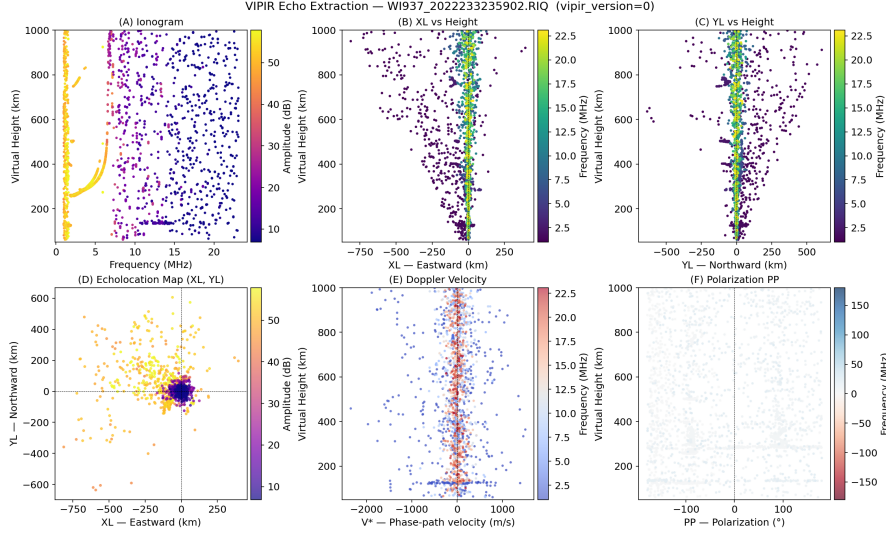


Figure 4: Six-panel diagnostic for WI937 echo extraction: ionogram (A), XL (B), YL (C), echo location map (D), Doppler V^* (E), PP (F).

Listing 3: Echo extraction and filtering

```
from pynasonde.vipir.riq.echo import EchoExtractor
from pynasonde.vipir.riq.parsers.filter import IonogramFilter

extractor = EchoExtractor(sct=riq.sct, pulsets=riq.pulsets,
                          snr_threshold_db=3.0).extract()
df = extractor.to_dataframe()

filtered = IonogramFilter(snr_threshold_db=6.0, ep_threshold_deg=30.0,
                          use_dbscan=True, use_ransac=True).fit(df)
```

4 Capon Cross-Spectrum Es Layer Imaging

4.1 Physical motivation

Sporadic-E (Es) layers are thin metallic-ion sheets at 90–130 km altitude. Their vertical thickness (< 1 km) is below the native range resolution of most ionosondes ($r_0 = 1.5\text{--}4$ km).

The pulse-compressed range profile $R_{ss}(t)$ is a complex sequence of V samples. Its FFT (the *cross-power spectrum*) is

$$G_{ss}(f_m) = \text{FFT}\{R_{ss}\}(f_m) = U(f_m) e^{j4\pi r f_m/c}, \quad (1)$$

where $U(f) = |S(f)|^2$ encodes signal power and the exponential encodes range r .

Liu et al. (2023) demonstrated 384 m resolution from a 3.84 km native gate using 256 pulses from the WISS digisonde.

4.2 Hankel subband matrix and covariance

Partition G_{ss} into a Hankel matrix \mathbf{G} of shape $(Z, V - Z + 1)$:

$$G[i, j] = G_{ss}[f_{i+j}], \quad i = 0 \dots Z - 1, j = 0 \dots V - Z. \quad (2)$$

The spatial covariance with diagonal loading ε :

$$\mathbf{R}_f = \frac{\mathbf{G}\mathbf{G}^H}{V - Z + 1} + \varepsilon \frac{\text{tr}(\mathbf{R}_f)}{Z} \mathbf{I}_Z. \quad (3)$$

4.3 Capon pseudospectrum

Steering vector $\mathbf{a}(\omega_\ell) \in \mathbb{C}^Z$ with $a_k(\omega_\ell) = e^{jk\omega_\ell}$ and $\omega_\ell = 2\pi\ell/(KV)$:

$$P\left(\frac{\ell r_0}{K}\right) = \frac{1}{\mathbf{a}^H(\omega_\ell) \mathbf{R}_f^{-1} \mathbf{a}(\omega_\ell)}, \quad \ell = 1, \dots, KV. \quad (4)$$

Effective range resolution: $\Delta r = r_0/K$.

4.4 Singularity constraints

\mathbf{R}_f has shape (Z, Z) and rank at most $V - Z + 1$. For full rank:

$$V - Z + 1 \geq Z \implies Z \leq \frac{V+1}{2}. \quad (5)$$

K has no singularity constraint. Earlier implementations incorrectly clipped $K \leq \lfloor V/Z \rfloor$; pynasonde ≥ 1.0 removes this constraint entirely.

Parameter roles:

Z Covariance size; affects rank of \mathbf{R}_f
 K Output grid only; does **not** enter \mathbf{R}_f

Liu et al. Fig. 1: $Z = 50$ (unresolved), $Z = 100$ (resolved, optimal), $Z = 150$ ($> (V+1)/2$, rank-deficient, partially recovered via diagonal loading).

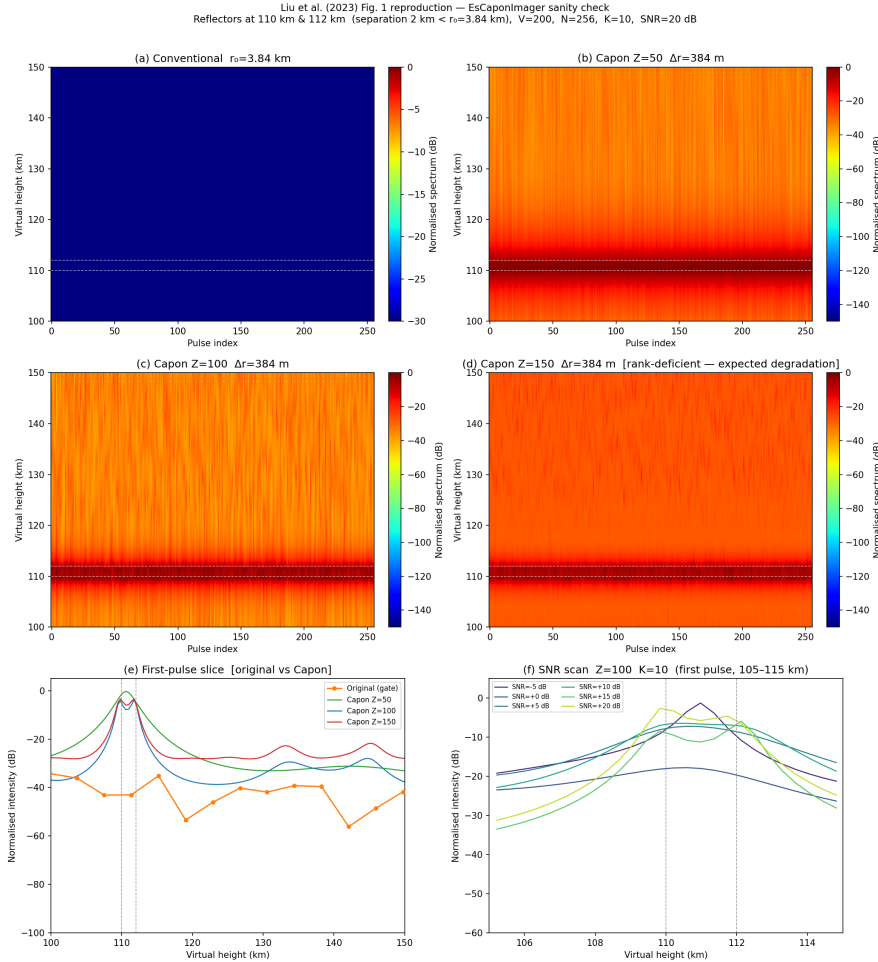


Figure 5: Synthetic sanity check reproducing Liu et al. (2023) Fig. 1. Two layers at 110 and 112 km ($r_0 = 3.84$ km, $V = 200$, $K = 10$). (a) Conventional; (b) $Z = 50$; (c) $Z = 100$; (d) $Z = 150$; (e) first pulse; (f) SNR scan.

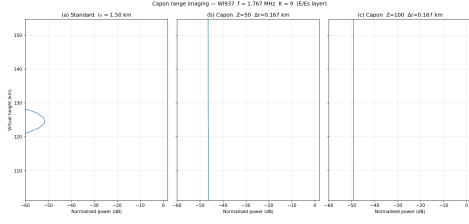


Figure 6: Single-file Es Capon image (1-D profile).

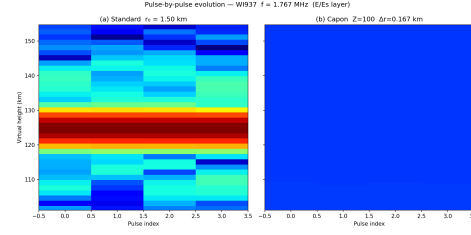


Figure 7: Slow RTI from RiqAggregator (A+B+C, 8 files).

Listing 4: EsCaponImager — single file

```
from pynasonde.vipir.analysis import EsCaponImager
imager = EsCaponImager(n_subbands=100, resolution_factor=10,
                        gate_spacing_km=1.499, gate_start_km=90.0)
result = imager.fit(iq_cube)
```

5 Multi-File A+B+C Combining (RiqAggregator)

5.1 Combining strategy

Option A — Coherent Rx beamforming:

$$R_{\text{beam}}[p, g] = \mathbf{S}[p, g, :] \mathbf{w}^*, \quad \Delta \text{SNR} = 10 \log_{10}(n_{rx}) \text{ dB}. \quad (6)$$

Option B — Incoherent pulse averaging (per file):

$$P_{\text{file}} = \frac{1}{n_p} \sum_p P_{\text{Capon}}(R_{\text{beam}}[p, :]). \quad (7)$$

Option C — Incoherent file stacking:

$$P_{\text{final}} = \frac{1}{n_f} \sum_f P_{\text{file}, f}. \quad (8)$$

Listing 5: RiqAggregator — multi-file A+B+C

```
from pynasonde.vipir.analysis import RiqAggregator
agg = RiqAggregator(n_subbands=100, resolution_factor=10,
                    output_mode="slow_rti") # or "single"
result = agg.fit(file_list, freq_target_khz=5000.0, freq_tol_khz=50.0)
```

Calibrated Rx weights from the antenna position table (SCT header `station.rx_position`) will be supported once the RIQ header reader exposes them.

SNR budget (8 files × 8 Rx):

Step

Opt. A (8 Rx)

Opt. B (4p avg)

Opt. C (8f stack)

Total

≈

6 HF Radio Absorption

No-field, weak-collision Appleton-Hartree absorption rate (dB km⁻¹):

$$\kappa(h) = \frac{4.343 \nu(h) X(h)}{c_{\text{km}} \sqrt{1 - X(h)}}, \quad X = (f_p/f)^2. \quad (9)$$

LOF index: $A = f_{\text{min}}^2 - f_{\text{ref}}^2$ [MHz²]. Differential O/X: $\Delta L(f) = \text{SNR}_O - \text{SNR}_X$ [dB].

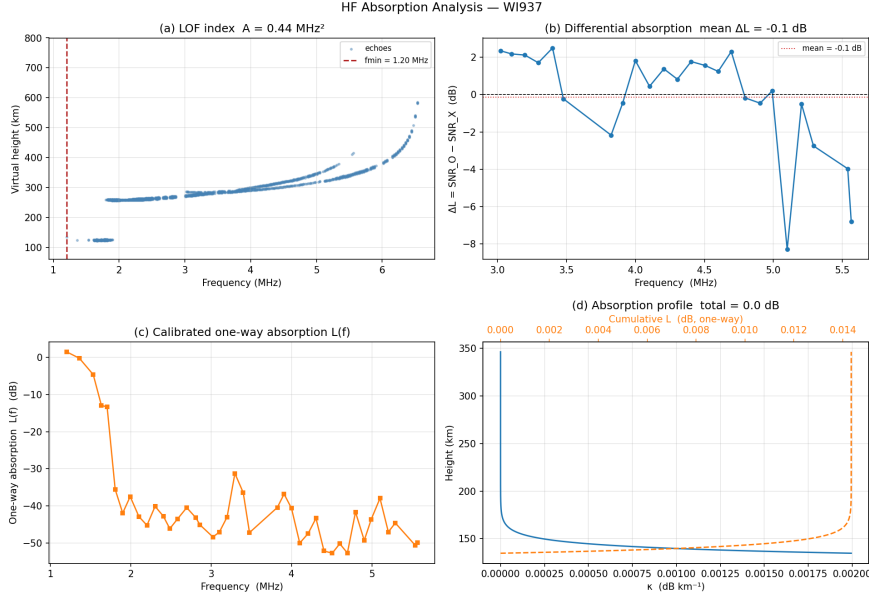


Figure 8: Absorption analysis panels: (a) LOF index, (b) differential O/X $\Delta L(f)$, (c) total calibrated $L(f)$, (d) height-resolved $\kappa(z)$.

Listing 6: AbsorptionAnalyzer — all four estimators

```
from pynasonde.vipir.analysis import AbsorptionAnalyzer
import numpy as np

aa = AbsorptionAnalyzer(f_ref_mhz=1.0)
lof = aa.lof_absorption(filtered_df)
diff = aa.differential_absorption(pol.annotated_df)
total = aa.total_absorption(filtered_df, tx_eirp_dbw=70.0)
calibrated = aa.calibrated
prof = aa.absorption_profile(edp, nu_hz=lambda h: 1e6*np.exp(-h/8.0))
# k(z)
```

7 True Height Inversion

The Titheridge (1967) lamination method discretises the Abel integral:

$$h_n = h'(f_n) - \sum_{j=1}^{n-1} (\mu'(f_n, f_j) - 1) \Delta h_j, \quad \mu'(f, f_p) = \frac{1}{\sqrt{1 - (f_p/f)^2}}. \quad (10)$$

Stability caveat: adjacent steps $< 0.1 \text{ MHz}$ cause near-singular μ' contr. pynasonde bins to ~ 0 before applying eq. (10) prescription).

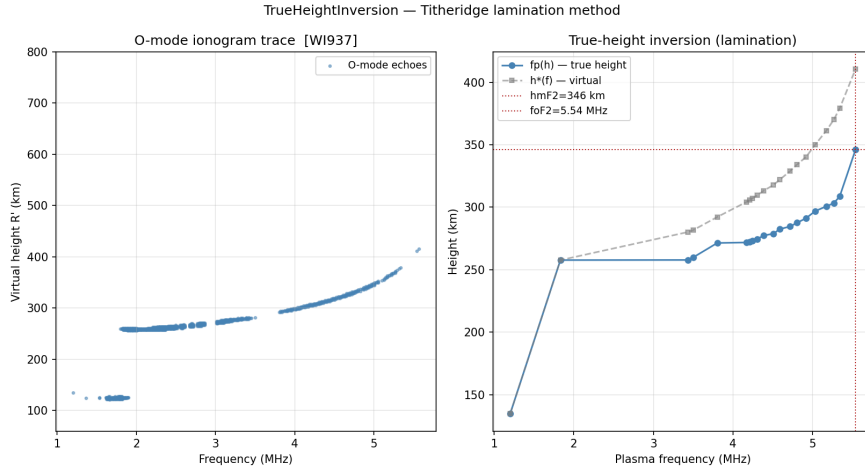


Figure 9: True height inversion output: $N(h)$ electron density profile (left) and virtual vs. true height comparison (right).

Listing 7: TrueHeightInversion API

```
from pynasonde.vipir.analysis import TrueHeightInversion
inv = TrueHeightInversion(monotone_enforce=True, bin_width_mhz=0.05)
edp = inv.fit_from_df(pol.annotated_df) # O-mode filter applied
                                         automatically
print(edp.summary()) # foF2=8.12 MHz hmF2=287.4 km NmF2=8.2e5 cm
                    ^-3
```

8 Polarization & Spread-F

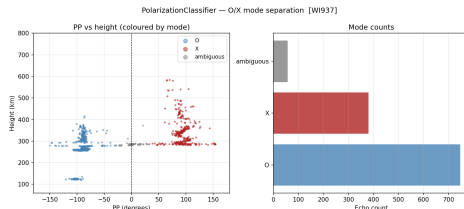


Figure 10: PP histogram with O/X classification regions.

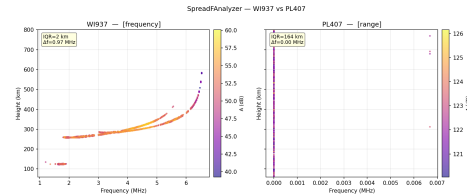


Figure 11: Spread-F detection: range/frequency/mixed type classification.

Listing 8: Polarization and Spread-F

```
from pynasonde.vipir.analysis import PolarizationClassifier,
SpreadFAnalyzer

pol = PolarizationClassifier(o_mode_sign=-1).fit(filtered_df)
sf = SpreadFAnalyzer().fit(filtered_df)
print(sf.summary()) # type=range foEs=4.2 MHz h_spread_km=38.1
```

9 Ionospheric Irregularity Analysis

9.1 Physical motivation

The EP (residual phase) parameter from the Dynasonde signal model carries information about sub-wavelength irregularities in the ionospheric reflection

layer. Irregularities imprint a structured signature on EP as a function of sounding frequency f .

9.2 Structure function approach

The second-order structure function of EP as a function of frequency lag Δf :

$$D_{EP}(\Delta f) = \langle [EP(f + \Delta f) - EP(f)]^2 \rangle. \quad (11)$$

For a power-law irregularity spectrum with spectral index α :

$$D_{EP}(\Delta f) \propto \Delta f^\alpha. \quad (12)$$

A log-log fit of D_{EP} vs Δf yields α and amplitude A_0 . The outer scale L_{outer} is estimated as the lag at which D_{EP} saturates.

9.3 Height-resolved and anisotropy analysis

Echoes are binned by virtual height, and the fit is computed independently per bin, giving a profile $\alpha(h)$. When both O-mode and X-mode EP are available:

$$\text{anisotropy proxy} = \frac{\sigma_{EP}(O)}{\sigma_{EP}(X)}. \quad (13)$$

A ratio near unity indicates isotropic scattering; deviations indicate field-aligned anisotropy.

Listing 9: IrregularityAnalyzer API

```
from pynasonde.vipir.analysis import IrregularityAnalyzer

irr = IrregularityAnalyzer(
    height_bin_km=10.0,      # virtual height bin width
    min_echoes_per_bin=5,    # minimum echoes for a valid fit
    lag_max=2.0,             # maximum frequency lag (MHz) for
                             # structure function
)
result = irr.fit(filtered_df)
# result.profile_df: columns = height_km, alpha, A0, outer_scale_km,
#                       anisotropy
# result.alpha_profile: 1-D alpha(h) array
# result.outer_scale_km: 1-D L_outer(h) array
result.plot_spectral_profile() # alpha(h) + outer scale overlay
result.plot_structure_function(height_km=200.0) # D_EP vs lag at one
# height
```

10 NeXtYZ 3-D Electron Density Inversion

10.1 Wedge-Stratified Ionosphere model

The NeXtYZ algorithm (Zabotin et al. 2006) represents the local electron density as a stack of plasma-frequency wedges bounded above by *frame planes*. Each wedge boundary is characterised by:

$$(h_{i+1}, n_{x,i+1}, n_{y,i+1}), \quad (14)$$

where h_{i+1} is the reflection height and (n_x, n_y) are the horizontal components of the outward normal — i.e., the ionospheric tilt.

*EP is the wavefront re
phase: the part of the
not explained by the n
group-range and Dopp
Random phase perturb
evidence of small-scale
irregularities.*

*NeXtYZ Lite solves o
wedge using constant
from mean angles of o
 $\approx 6\times$ faster than Full
sufficient for moderate*

10.2 Hamiltonian eikonal ray tracing

Signal propagation through the WSI model is computed via the eikonal (method of characteristics) equations:

$$\dot{\mathbf{r}} = \partial H / \partial \mathbf{k}, \quad (15)$$

$$\dot{\mathbf{k}} = -\partial H / \partial \mathbf{r}, \quad (16)$$

with Hamiltonian $H = |\mathbf{k}|^2 - n^2(\mathbf{r}, f)$ and the full Appleton-Lassen refractive index n .

10.3 Inversion loop

Wedge parameters are solved bottom-up by alternately minimising:

1. **Group-range residual:** $\Delta R'_{i+1} = \sqrt{\sum_j (\rho'_{i+1,j} - R'_{i+1,j})^2}$
2. **Ground-return distance** of the mean-direction ray (tilt constraint).

Listing 10: NeXtYZInverter API

```
from pynasonde.vipir.analysis import NeXtYZInverter, NeXtYZResult

inv3d = NeXtYZInverter(
    mode="lite",           # "lite" (fast, const tilts) or "full" (per-
                          # wedge tilts)
    n_wedge_max=30,        # maximum number of WSI wedge layers
    ray_step_km=0.5,       # Hamiltonian integrator step size
    tilt_regularisation=0.01, # weight of tilt constraint vs group-
                          # range fit
)
result: NeXtYZResult = inv3d.fit(filtered_df)

# Key output attributes
print(result.fp_profile)   # plasma frequency vs true height
print(result.tilt_x)       # E-W tilt per wedge (degrees)
print(result.tilt_y)       # N-S tilt per wedge (degrees)
print(result.height_error_km) # estimated layer height uncertainty

result.plot_wedge_planes() # 3-D visualisation of WSI frame planes
result.plot_fp_profile()  # fp(h) vs true height
```

11 API Quick-Reference

11.1 All public imports

```
# DIGISONDE I/O
from pynasonde.digisonde.parsers.sao import SaoExtractor,
    SaoSummaryPlots
from pynasonde.digisonde.parsers.rsrf import RsfExtractor
from pynasonde.digisonde.parsers.sbf import SbfExtractor
from pynasonde.digisonde.parsers.dft import DftExtractor
from pynasonde.digisonde.parsers.dvl import DvlExtractor
from pynasonde.digisonde.parsers.sky import SkyExtractor,
    SkySummaryPlots
from pynasonde.digisonde.parsers.edp import EdpExtractor

# VIPIR I/O
from pynasonde.vipir.rsq.parsers.read_rsq import RsqDataset,
    VIPIR_VERSION_MAP
from pynasonde.vipir.rsq.echo import EchoExtractor
from pynasonde.vipir.rsq.parsers.filter import IonogramFilter
from pynasonde.vipir.ngi.source import DataSource
from pynasonde.vipir.ngi.scale import AutoScaler
```

```

# Analysis layer
from pynasonde.vipir.analysis import (
    PolarizationClassifier, PolarizationResult,
    TrueHeightInversion, EDPResult,
    AbsorptionAnalyzer, LOFResult, DifferentialResult,
    TotalAbsorptionResult, AbsorptionProfileResult,
    SpreadFAnalyzer, SpreadFResult,
    IrregularityAnalyzer, IrregularityProfile,
    IonogramScaler, ScaledParameters,
    EsCaponImager, RiqAggregator, EsImagingResult,
    NeXtYZInverter, NeXtYZResult, WedgePlane,
)

```

11.2 Constructor summary

Table 2: Key constructor parameters for all analysis classes.

Class	Parameter	Default	Notes
EsCaponImager	n_subbands	100	Z ; recommended $\leq (V+1)/2$
	resolution_factor	10	K ; no singularity limit
	gate_spacing_km	3.84	r_0 ; VIPIR WI937 = 1.499 km
	diagonal_loading	1e-3	ε for \mathbf{R}_f conditioning
RiqAggregator	rx_weights	None	None = uniform $1/n_{rx}$
	output_mode	single	or <code>slow_rti</code>
	gate_spacing_km	1.499	overridden from RIQ header
TrueHeightInversion	method	lamination	only supported method
	bin_width_mhz	0.05	trace decimation for stability
	monotone_enforce	True	remove non-monotone layers
AbsorptionAnalyzer	f_ref_mhz	1.0	quiet-day reference for LOF
PolarizationClassifier	o_mode_sign	-1	+1 for southern hemisphere
IrregularityAnalyzer	height_bin_km	10.0	virtual height bin width
	min_echoes_per_bin	5	minimum for valid power-law fit
	lag_max	2.0 MHz	max frequency lag for D_{EP}
NeXtYZInverter	mode	lite	lite (fast) or full (per-wedge tilts)
	n_wedge_max	30	maximum WSI wedge layers
	ray_step_km	0.5	Hamiltonian integrator step size
	tilt_regularisation	0.01	tilt constraint weight

11.3 Result dataclasses at a glance

Table 3: Key attributes of result objects.

Class	Key attributes	Shape
EsImagingResult	pseudospectrum.db heights.km effective_resolution.km	(n_s, KV) $(KV,)$ scalar
EDPResult	true_height.km, plasma_freq.mhz foF2.mhz, hmF2.km, NmF2.cm3	$(n_L,)$ scalar
AbsorptionProfileResult	profile.df (h, ν, f_p, X, κ) total_absorption.db	DataFrame scalar
PolarizationResult	annotated.df (mode column) o_mode_count, x_mode_count	DataFrame int

References

- Liu, T., Yang, G., & Jiang, C. (2023). High-resolution sporadic E layer observation. *Space Weather*, 21, e2022SW003195. <https://doi.org/10.1029/2022SW003195>
- Titheridge, J. E. (1967). *JATP*, 29, 763–778.
- Paul, A. K. (1975). POLAN. *NOAA Technical Report ERL 324-SEL 31*.
- Zaboltn, N. A., Wright, J. W., & Zhbankov, G. A. (2006). NeXtYZ. *Radio Science*, 41, RS6S32.
- Davies, K. (1990). *Ionospheric Radio*. Peter Peregrinus.
- Budden, K. G. (1985). *The Propagation of Radio Waves*. Cambridge.
- Grubb, R. N., et al. (2011). New science with VIPIR. *Radio Science*.
- Reinisch, B. W., et al. (1997). The Digisonde 4D. *JASTP*, 59, 2181.